ChemComm

Accepted Manuscript

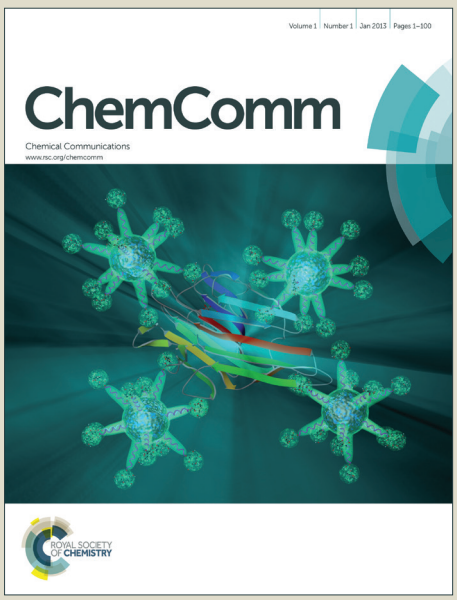

ROYAL SOCIETY OF CHEMISTRY

www.rsc.org/chemcomm

Journal Name

RSCPublishing

COMMUNICATION

Visualization of nitroxyl (HNO) *in vivo* via a lysosome-targetable near-infrared fluorescent probe

Cite this: DOI: 10.1039/x0xx00000x

Xiaotong Jing,[a,b†] Fabiao Yu[b†] and Lingxin Chen*[b]

Received 00th January 2012,
Accepted 00th January 2012

DOI: 10.1039/x0xx00000x

www.rsc.org/

We have presented a near-infrared fluorescent probe Lyso-JN for the detection of nitroxyl (HNO) in cells and in vivo. Lyso-JN is comprised of three moieties: an Aza-BODIPY fluorophore, a HNO-response modulator diphenylphosphino-benzoyl, and a lysosomal locator alkylmorpholine. The detection mechanism is based on aza-ylide intramolecular ester aminolysis reaction upon reaction with HNO. The probe holds ability to capture lysosomal HNO in RAW 264.7 cells, and also successfully employed to visualize HNO in mice.

To date, the reactive nitrogen species (RNS) have received considerable attention. Many remarkable achievements have been established due to their vital roles in special functions during the physiological and pathological processes.[1] As the "Ugly Duckling" of RNS, the roles of nitroxyl (HNO) are among the least thoroughly investigated. The relevant investigations reveal that HNO possesses unique and potential bio-pharmacological effects which distinguish it from NO.[2] As an electrophile, HNO can resist superoxide infraction in mammalian vascular systems.[3] However, HNO also behaves a nucleophile to coordinate and reduce metal ions.[4] More importantly, HNO can increase systolic force and decrease diastolic pressure in both normal and failing canine hearts through upregulating calcitonin gene-related peptide.[5] Thus, more and more examinations suggest that HNO may provide a powerful therapeutic agent for heart failure cure. Despite biochemical studies have proposed some biosynthetic pathways, for instance, HNO can be formed directly from NO and H_2S via a redox reaction.[6] The mechanisms of HNO formation are still not elucidatived clearly because of the lack of efficacious detection tools. Therefore, the development of reliable methods for HNO detection remains a challenging task.

Being an important organelle, lysosomes play vital roles in regulating cellular metabolic capabilities, which involve in accepting intracellular cargo from each autophagy.[7] Some examples pioneered that NO can react with several related proteins outside lysosomes to launch the autolysosome process.[8] Coupled with an interconversion between HNO and NO in the presence of superoxide dismutase,[9] it is reasonable to anticipate that HNO may have some bioeffects on the components of lysosomes during physiological processes.

HNO always exhibits high chemical reactivity in biological systems. The rapid dimerization and dehydration to nitrous oxide (N_2O) always hamper the accurate detection of HNO in cells and in vivo.[10] Taking advantage of the high sensitivity, non-invasiveness and high spatiotemporal resolution for visualizing bioreactive species in biological system, fluorescence probes are the preferred candidates to elucidate the mechanisms of these species.[11] Recently, a few Cu^{2+}-mediated fluorescent probes have been developed for the detection of HNO.[12] However, the above-mentioned fluorescent probes are prone to be interfered by biological reductants such as ascorbic acid and glutathione (GSH). Some studies establish that HNO can react with triarylphosphine to give the corresponding phosphine oxide and aza-ylide. The aza-ylide will undergo an immediate aza-ylide intramolecular ester aminolysis reaction to release alcohol and amide.[13] This reaction may provide a promising opportunity for HNO detection chemically.[14] Despite the new development of HNO detection, there still lacks of organelle-targeted fluorescent probes. Especially the probes' absorption and emission locate in the near-infrared (NIR) region which can penetrate tissues more deep and avoid background noise.[15]

To solve above problems, we invested effort into developing a lysosome-targetable NIR fluorescent probe Lyso-JN for visualization of HNO in cells and in vivo. As shown in Scheme1, the fluorescent probe Lyso-JN is consisted of three moieties: i) A BF_2-chelated tetraarylazadipyrromethane fluorophore (Aza-BODIPY) whose absorption/emission wavelengths locates in NIR spectral region. The fluorophore also features as good resistance to photobleaching, high fluorescence quantum yield, and good membrane permeability. ii) The HNO recognition unit diphenylphosphinobenzoyl group, which reacts with HNO to form

aza-ylide. Aza-ylide will nucleophilically attack on the carbonyl of the ester, resulting in the release of Lyso-1. iii) The lysosomal locator alkylmorpholine, which possesses a typical lysosome-targeting function, and have been widely incorporated into compounds to realize the lysosome-targetable cability.[16] All these features guarantee Lyso-JN feasibly to capture HNO in lysosomes. We now developed a versatile fluorescent probe for HNO detection in lysosomes. The synthesis of the probe was shown in support information (ESI†). The following experimental results proved that Lyso-JN could offer good performances in terms of sensitivity, selectivity, and low cytotoxicity.

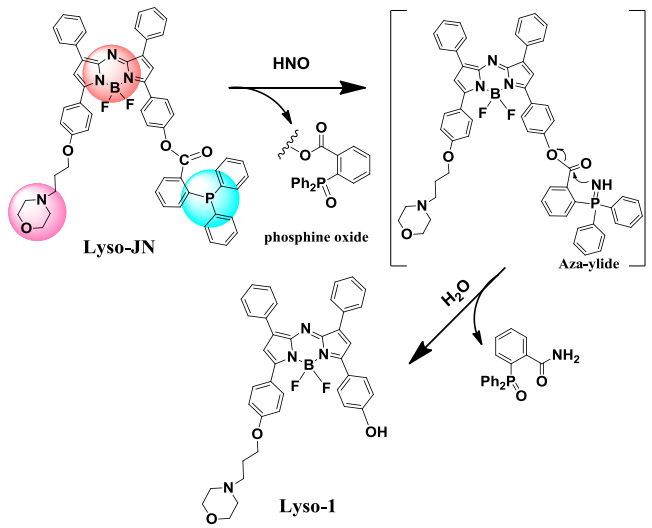

Scheme 1 Structure and reaction mechanism of the probe **Lyso-JN**.

The fluorescence intensity at various pHs were performed to demonstrate the potential behaviors of our probe Lyso-JN (HEPES buffer solution 10 mM, 0.5% DMSO, 0.5% TW 80). The pHs hardly have effects on the fluorescence intensity of Lyso-JN. The fluorescence intensity of Lyso-1 stayed at a higher level before pH 6.0 (Fig. S2, ESI†). Considering the physiological pH of lysosomes was at 4.5−5.5, our probe Lyso-JN would be suitable for applications in lysosome.

We investigated the spectroscopic properties of probe Lyso-JN in HEPES buffer solution (10 mM, 0.5% DMSO, 0.5% TW 80, pH 5.0). Upon addition of Angeli's salt (AS, a HNO donor), the fluorescence intensity of Lyso-JN enhanced apparently with a maximum at 700 nm (Fig.1a). The quantum yields of Lyso-JN increased from 0.01 to 0.37 (see ESI†). These results manifested that Lyso-JN was a turn-on type fluorescent probe for HNO detection. There was a good linearity between relative fluorescent intensity at 700 nm and the concentrations of AS ranging from 0 – 10 μM (Fig.1b). The regression equation was $F_{700\ nm}$ =34.88 [AS] (μM) -39.84 (r= 0.995). The detection limit (S/N=3) toward HNO was calculated to be 0.06 μM, suggesting that Lyso-JN was highly sensitive to HNO. The absorption spectra of Lyso-JN was examined at the same conditions as above mentioned. Lyso-JN exhibited an absorption maximum at 684 nm (ε = 4.05 × 10^4 $M^{-1}cm^{-1}$) (Fig. S3, ESI†). The probe showed λ_{max} and emission both in the NIR region, indicating that Lyso-JN was potential for application in cells and in vivo.

We next evaluated the selectivity of Lyso-JN towards HNO across a serious of other related species in biological systems. Lyso-JN was incubated with various biologically relevant species including S-nitrosoglutathione (GSNO), $ONOO^-$, NO (NOC-5), NO_2^-, tocopherols, H_2O_2, O_2^-, methyl linoleate hydroperoxide (MeLOOH), ClO^-, *L*-Cysteine (L-cys), GSH, NaHS, ascorbic acid, citrate, tyrosine (Tyr) and hydroxylamine (HA) (Fig.2). During 0, 5, 10, 15, and 20 min, HNO induced a remarkable fluorescence enhancement with an excitation at 690 nm. As is well-known, AS can decompose readily to generate HNO and NO_2^- at above pH 4.0 (see ESI†). While the probe was treated with 500 μM $NaNO_2$, there was no influence toward fluorescence (Fig.2b). The results verified that the fluorescence response induced by AS was due to HNO rather than the byproduct. When biological reductants, such as GSH, ascorbic acid and NaHS were added to the HEPES buffer solution, no obvious fluorescence signals were found. GSNO was reported to react with triarylphosphines, generating similar phosphine oxide and aza-ylide.[17] Nevertheless, as Fig. 2a displayed, the change of fluorescence caused by GSNO was comparatively slightly, which revealed that the reaction between GSNO and Lyso-JN was obviously weaker than that of HNO. Lyso-JN was better selectivity to HNO over GSNO. Together, these results indicated that Lyso-JN possess excellent selectivity in the presence of various biologically relevant species.

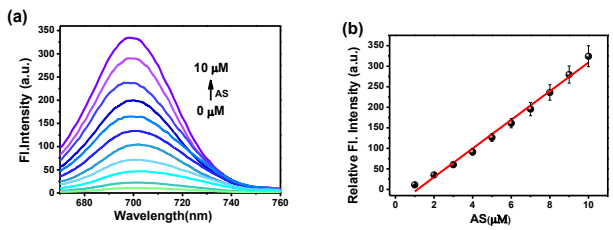

Fig.1 (a) Fluorescence responses of Lyso-JN (2 μM) to different concentrations of Angeli's salt (AS) with emission ranging from 670 to 760 nm. λ_{ex}= 690 nm. (b) Relationship between the relative fluorescence intensity at 700 nm and concentrations of AS (0, 1, 2, 3, 4, 5, 6, 7, 8, 9, 10 μM). Fluorescence spectra were acquired in HEPES buffer solution (10 mM, 0.5% DMSO, 0.5% TW 80, pH 5.0).

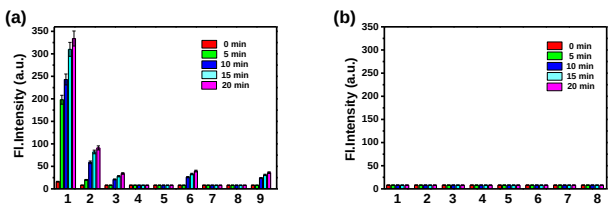

Fig. 2 (a) Time-dependent fluorescence response of 2 μM Lyso-JN to the testing species in HEPES buffer solution (10 mM, 0.5% DMSO, 0.5% TW 80, pH 5.0): 1, 10 μM AS; 2, 20 μM GSNO; 3, 200 μM $ONOO^-$; 4, 50 μM NOC-5; 5, 500 μM NO_2^-; 6, 200 μM H_2O_2; 7, 100 μM O_2^-; 8, 20 μM MeLOOH; 9, 200 μM ClO^-. (b) 1, 50 μM L-cys; 2, 100 μM GSH; 3, 500 μM NaHS; 4, 200 μM ascorbic acid; 5, 200 μM tocopherols; 6, 100 μM citrate; 7, 200 μM tyrosine (Tyr); 8, 50 μM hydroxylamine (HA). Bars represent fluorescence intensity during 0, 5, 10, 15, and 20 min after addition of various compounds. λ_{ex}= 690 nm, λ_{em}= 700 nm.

Most lysosomal probes which modified with alkaline groups can induce pH increases in lysosome and lead to cell apoptosis. Therefore, we performed a standard MTT assay to evaluate the cytotoxicity of Lyso-JN. The results showed that cell viability was over 80% even though 100 μM Lyso-JN was added for 24 h (Fig. S5, ESI†), indicating that Lyso-JN had a low cytotoxicity.

The multicolor colocalization method that based on analysis of spectrally separated images and the simultaneous acquisition enable measure molecular distances with accuracy better than 10 nm.[18] Next, we investigated the ability of Lyso-JN for HNO detection in living cells (Experimental details in ESI†). Initially, RAW264.7 cells were incubated with 10 μM Lyso-JN for 30 min at 37 °C. As control, the cells showed faint fluorescence in Fig. 3a. However, when incubated with 200 μM AS for 20 min, the cells displayed apparent levels of fluorescence in cells (Fig. 3b). The time-dependent fluorescence intensity of Lyso-JN within 60 min was shown in Fig. 3c. The fluorescence intensity raised to a plateau within 30 min, and featured a 38-fold fluorescent enhancement, describing the good light stability and strong fluorescence enhancement of Lyso-JN in living cells. These results indicated that Lyso-JN was available for detection of HNO in living cells.

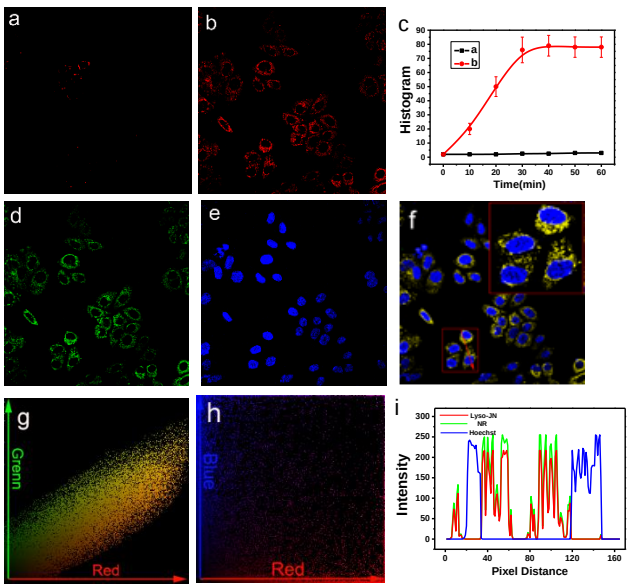

Fig. 3 Fluorescence confocal microscopic imaging for Lyso-JN, NR and Hoechst. (a) control; (b) 10 μM Lyso-JN (red channel : λ_{ex} = 635 nm, λ_{em}= 700–800 nm); (c) Time-dependent fluorescence intensity of Lyso-JN in (a) and (b); (d) 2 μM NR showing lysosomes (green channel: λ_{ex} = 559 nm, λ_{em} = 570–650 nm); (e) 2 μM Hoechst showing nuclei (blue channel: λ_{ex} = 405nm, λ_{em} =425 – 525nm); (f) overlay of (b), (d) and (e); (g) Displayed the colocalization areas of the red and green channels selected; (h) Displayed the colocalization areas of the red and blue channels selected; (i) Intensity profile of regions of interest (red arrow in Fig. 3f) across RAW264.7 cells. Scale bar = 20 μm.

In order to examine Lyso-JN's lysosomes-targeting ability, we carried out colocalization experiment by costaining RAW264.7 with Neutral Red (NR, a commercial LysoTracker) and nuclear stain Hoescht 33342. RAW264.7 cells were loaded with 2 μM Hoechst for 10 min before staining with 10 μM Lyso-JN for 5 min. And then the cells were treated with 200 μM AS for 20 min. Finally, 2 μM NR was added and the cells were incubated for another 5 min at 37°C. As shown in Fig. 3f, the fluorescence image of Lyso-JN (Fig. 3b) overlapped with that of the NR (Fig. 3d) in discrete subcellular locations. Blue fluorescence displayed well in cell nucleus (Fig.3e). Besides, the intensity profiles of the linear regions of interest (red arrow in Fig. 3f) across RAW264.7 cells stained with Lyso-JN and NR altered in close synchrony (Fig. 3i). The dependent staining of Lyso-JN and NR in Fig. 3g resulted in highly correlated plots. However, the correlation of Lyso-JN and Hoescht 33342 exhibited a discrete fluorescence (Fig.3h, 3i). These results successfully indicate that Lyso-JN can exclusively localize in lysosomes. Taken together, we have successfully demonstrated that Lyso-JN could be lysosome-targetable and suitable for the detection of HNO in living cells.

We further applied Lyso-JN for HNO imaging in the BALB/c mice (n=5). Group in mice 1 were injected with 50 μM Lyso-JN (50 μL in 1:9 DMSO/saline v/v), and 10 min later, the mice 1 was given 1 mM AS (50 μL in saline) in the same region. After 30 min, there exhibited a remarkable increase fluorescence in the full abdominal cavity (Fig. 4a). For the control, group in mice 2 showed only faint fluorescence. These results showed that the NIR fluorescent probe Lyso-JN could be successfully applied for deep imaging in live mice and effectively avoided organisms' autofluorescence. In addition to the aforementioned fluorescence imaging, merging with X-ray imaging could also clearly displayed the definite light-emitting parts of the mice (Fig. 4b, Fig. S8 ESI†). The quantification of mean fluorescence intensity of each group was shown in Fig.4c. It was noteworthy that the total number of photons from the entire peritoneal cavity was ~7.5-fold than that of control. Above experiments demonstrated that Lyso-JN achieved the noninvasive imaging in living mice and was sensitive enough to visualize HNO in living animals.

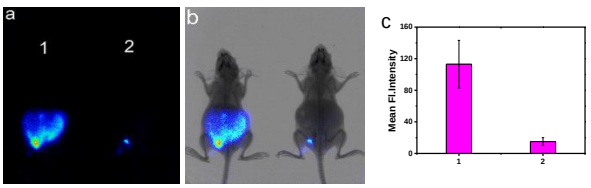

Fig. 4 Fluorescence/X-ray imaging in peritoneal cavity of the BALB/c mice. (1) Mice injected i.p. with Lyso-JN (50 μM, 50 μL in 1:9 DMSO/saline v/v), and then loaded with AS (1 mM, 50 μL in saline) for more 30 min. (2) Mice injected i.p. with Lyso-JN (50 μM, 50 μL in 1:9 DMSO/saline v/v) for 40 min. (a) Fluorescence imaging ; (b) merged fluorescence imaging with X-ray imaging; (c) Quantification of total photon flux from region of interest measurement of each group. n = 5, error bars are ± SD. Images constructed from 670 nm fluorescence window, λ_{ex}= 660 nm.

In summary, we develop a new NIR fluorescent probe Lyso-JN for HNO detection in macrophage cells and in mice. Lyso-JN exhibits high selectivity, good sensitivity and low cytotoxicity when detect HNO. Besides, the probe shows perfect lysosomal localization in living cells. We confirm that Lyso-JN can detect HNO in mice without interference from background fluorescence. The probe Lyso-JN may present a promising tool to research lysosomal HNO during the physiological and pathological processes.

We thanks NSFC (NO.21405172, No.21275158), the Innovation Projects of the CAS (Grant KZCX2-EW-206), and the program of Youth Innovation Promotion Association, CAS.

Notes and references

†These authors contributed equally.
[a]The Key Laboratory of Life-Organic Analysis, College of Chemistry and Chemical Engineering, Qufu Normal University, Qufu 273165, China.
[b]Key Laboratory of Coastal Environmental Processes and Ecological Remediation; The Research Center for Coastal Environmental Engineering and Technology, Yantai Institute of Coastal Zone Research, Chinese Academy of Sciences (CAS), Yantai 264003, China.
Email: lxchen@yic.ac.cn

† Electronic supplementary information (ESI) available: Synthesis procedures and experimental details. See DOI: 10.1039/x0xx00000x

1 (a) X. Chen, X. Tian, I. Shin and J. Yoon, *Chem. Soc. Rev.*, 2011, **40**, 4783-4804; (b) Y. Yang, Q. Zhao, W. Feng and F. Li, *Chem. Rev.*, 2013, **113**, 192-270; (c) T, Nagano., *J. Clin. Biochem. Nutr.*, 2009, **45**, 111-124; (d) J. Chan, S. C. Dodani and C.J. Chang, *Nat. Chem.*, 2012, **4**, 973-984.

2 (a) J. M. Fukuto, C. J. Cisneros and R. L. Kinkade, *J. Inorg. Biochem.*, 2013, **118**, 201−208; (b) M. G. Espey, K. M. Miranda, D. D. Thomas and D. A. Wink, *Free. Radical. Bio. Med.*, 2002, **33**, 827–834.

3 G. Keceli and J. P. Toscano, *Biochemistry*, 2012, **51**, 4206–4216.

4 J. M. Fukuto and S. J. Carrington, *Antioxid. Redox. Signal.*, 2011, **14**, 1649−1657.

5 N. Paolocci, T. Katori, H.C. Champion, M.E. St John, K.M. Miranda, J.M. Fukuto, D. A. Wink and D.A. Kass., *Proc. Natl. Acad. Sci. USA.*, 2003, **100**, 5537–5542.

6 M. Eberhardt, M. Dux, B. Namer, J. Miljkovic, N. Cordasic, C. Will, T.I. Kichko, J.de la Roche, M. Fischer, S.A. Suárez, D. Bikiel, K. Dorsch, A. Leffler, A. Babes, A. Lampert, J. K. Lennerz, J. Jacobi, M.A. Martí, F. Doctorovich, E.D. Högestätt, P. M. Zygmunt, I. vanovic-Burmazovic, K. Messlinger, P. Reeh and M. R. Filipovic, *Nat. Commun.*, 2014, **5**, 4381.

7 J. D. Rabinowitz and E. White, *Science*, 2010, **330**, 1344−1348.

8 T. R. M. da Silva, J. R. de Freitas, Q. C. Silva, C. P. Figueira, E. Roxo, S. C. Leao, L. A. R. de Freitas and P. S. T. Veras, *Infect. Immun.*, 2002, **70**, 5628−5634.

9 M. E. Murphy and H. Sies, *Proc. Natl. Acad. Sci. U.S.A.*, 1991, **88**, 10860−10864.

10 (a) A. S. Dutton, J. M. Fukuto and K. N. Houk, *J. Am. Chem. Soc.*, 2004, **126**, 3795-3800; (b) N. Paolocci, M. I. Jackson, B. E. Lopez, K. Miranda, C. G. Tocchetti, D. A. Wink, A. J. Hobbs and J. M. Fukuto, *Pharmacol. Ther.*, 2007, **113**, 442-458; (c) J. C. Irvine, R.H. Ritchie, J. L. Favaloro, K. L. Andrews, R. E. Widdop and B. K. Kemp-Harper, *Trends. Pharmacol. Sci.*, 2008, **29**,601-608.

11 (a) J. Fan, M. Hu, P. Zhan and X. Peng, *Chem. Soc. Rev.*, 2013, **42**, 29-43; (b) X. Li, X. Gao, W. Shi and H. Ma, *Chem. Rev.*, 2014, **114**, 590-659; (c) F. Yu, X. Han and L. Chen, *Chem. Commun.*, 2014, **50**, 12234-12249; (d) R. Wang, C. Yu, F. Yu and L. Chen, *Trends. Anal. Chem.* 2010, **29**, 1004-1013.

12 (a) J. Rosenthal and S. J. Lippard, *J. Am. Chem. Soc.*, 2010, **132**, 5536-5537; (b) U.P. Apfel, D. Buccella, J. J. Wilsona and S. J. Lippard, *Inorg. Chem.*, 2013, **52**, 3285-3294; (c) Y. Zhou, K. Liu, J. Li, Y. Fang, T. Zhao and C. Yao, *Org. Lett.*, 2011, **13**, 1290-1293; (d) A.T. Wrobel, T.C. Johnstone, Liang. A. Deliz, S. J. Lippard and P. Rivera-Fuentes, *J. Am. Chem. Soc.*, 2014, **136**, 4697-4705; (e) Y. Zhou, Y. Yao, J. Li, C. Yao and B. Lin, *Sens. Actuators. B. Chem.*, 2012,**174**, 414–420.

13 (a) J.A. Reisz, C.N. Zink and S.B. King, *J. Am. Chem. Soc.*, 2011, **133**, 11675-11685; (b) J.A. Reisz, E.B. Klorig, M.W. Wright and S.B. King, *Org. Lett.*, 2009, **11**, 2719-2721.

14 (a) K. Kawai, N. Ieda, K. Aizawa, T. Suzuki, N. Miyata and H. Nakagawa, *J. Am. Chem. Soc.*, 2013,**135**,12690-12696; (b) G. Mao, X. Zhang, X. Shi, H. Liu, Y. Wu, L. Zhou, W. Tan and R. Yu, *Chem. Commun.*, 2014, **50**, 5790-5792; (c) C. Liu, H. Wu, Z. Wang, C. Shao, B. Zhu and X. Zhang, *Chem. Commun.*, 2014, **50**, 6013-6016.

15 L. Yuan, W. Lin, K. Zheng, L. He and W. Huang, *Chem. Soc. Rev.*, 2013, **42**, 622-661.

16 (a) Q. Wan, S. Chen, W. Shi, L. Li and H. Ma, *Angew. Chem. Int. Ed.*, 2014, doi: 10.1002/ange.201405742; (b) H. Yu, Y. Xiao and L. Jin. *J. Am. Chem. Soc.*, 2012, **134**, 17486-17489; (c) T. J. Rink, R. Y. Tsien and T.J. Pozzan, *Cell. Biol.*, 1982, **95**, 189−196.

17 (a) E. Bechtold, J. A. Reisz, C. Klomsiri, A.W. Tsang, M.W. Wright, L.B. Poole, C.M. Furdui and S.B. King, *ACS. Chem. Biol.*, 2010, **5**, 405-414; (b) D. Zhang, W. Chen, Z. Miao, Y. Ye, Y. Zhao, S.B. King and M. Xian, *Chem. Commun.*, 2014, **50**, 4806-4809.

18 X. Michalet, T. D. Lacoste and S. Weiss, *Methods.*, 2001, **25**, 87-102.

